ORGANOMETALLICS

pubs.acs.org/Organometallics Article

Thermochemical Studies of Nickel Hydride Complexes with Cationic Ligands in Aqueous and Organic Solvents

Andrew D. Cypcar, Tyler A. Kerr, and Jenny Y. Yang*



Cite This: Organometallics 2022, 41, 2605-2611



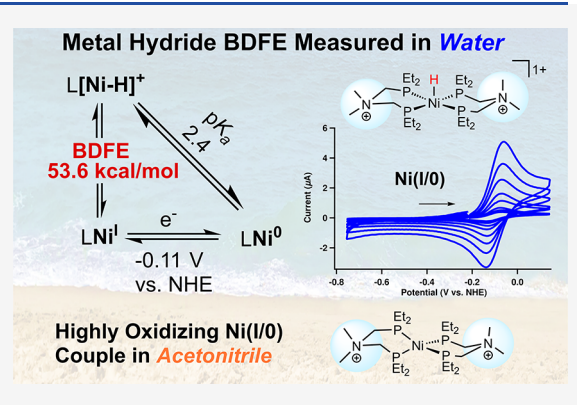
ACCESS

III Metrics & More

Article Recommendations

s Supporting Information

ABSTRACT: Transition metal hydride complexes are key intermediates in a variety of catalytic processes. Transfer of a hydride, hydrogen atom, or proton is defined by the thermochemical parameters of hydricity, bond dissociation free energy (BDFE), and pK_a , respectively. These values have been studied primarily in organic solvents to predict or understand reactivity. Despite growing interest in the development of aqueous metal hydride catalysis, BDFE measurements of transition metal hydrides in water are rare. Herein, we report two nickel hydride complexes with one or two cationic ligands that enable the measurement of BDFE values in both aqueous and organic solvents using their reduction potential and pK_a values. The Ni(I/0) reduction potentials increase anodically as more charged groups are introduced into the ligand framework and are among the most positive values measured for Ni complexes. The complex with two



cationic ligands, 2-Ni(II)—H, displays exceptional stability in water with no evidence of decomposition at pH 1 for at least 2 weeks. The BDFE of the nickel hydride bond in 2-Ni(II)—H was measured to be 53.6 kcal/mol in water and between 50.9 and 56.2 kcal/mol in acetonitrile, consistent with prior work that indicates minimal solvent dependence for BDFEs of O—H and N—H bonds. These results indicate that transition metal hydride BDFEs do not change drastically in water and inform future studies on highly cationic transition metal hydride complexes.

INTRODUCTION

Transition metal hydride complexes are common intermediates in catalytic reductions and can react as hydride, H-atom, or proton donors. For example, in one of the simplest reductions, the hydrogen evolution reaction (HER), electrocatalysts are known to form H–H bonds either through a heterolytic mechanism through protonation of a metal hydride or through homolytic bond formation, where H-atoms from two M–H complexes combine to form H₂ and two reduced metal centers. Additionally, metal hydrides are implicated in CO₂ reduction reactions and organic transformations, such as hydrogenations and radical hydrofunctionalization reactions.

The thermodynamic parameters of a metal hydride—hydricity, pK_a , and BDFE (bond dissociation free energy)—define the free energies for hydride transfer, proton transfer, and hydrogen atom transfer (HAT), respectively. These values are interrelated through square schemes (Figure 1a). For metal hydrides, these values have been most commonly studied in organic solvents, particularly acetonitrile (MeCN). Nature 4,10,11 In water, pK_a values of approximately 20 transition metal hydrides have been documented, and there has been more recent interest in evaluating aqueous hydricity values. However, there is a notable lack of transition metal hydride BDFEs that have been measured in water. Most prominent is the work of Wayland and co-workers, where equilibrium measurements

were used to obtain estimates of BDFEs in metal porphyrin complexes. 16,17

Measuring BDFEs of metal hydrides in water presents unique challenges (Figure 1b). Protonation of a metal hydride by protons in water to form H_2 and the corresponding oxidized metal is often favorable. To obtain a BDFE value using a square scheme, an accurate pK_a value and one electron reduction potential are needed (Figure 1a). However, the narrow pH range of water limits the range of measurable pK_a values, and most transition metal complexes exhibit irreversible redox events in water. The BDFE value could also be measured by equilibrium measurements with H-atom donors/acceptors with known BDFE values close to the value of a metal hydride. Yet, few H-atom donor/acceptors with suitable BDFEs have been reported in water, and some of these favor spontaneous H_2 evolution through homolytic bond formation. ¹⁸

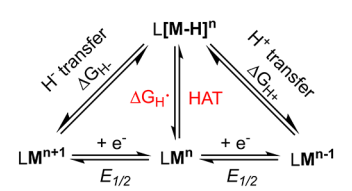
In order to elucidate a more complete understanding of aqueous metal hydride thermochemistry and how it relates to

Received: June 28, 2022 Published: September 13, 2022





a. Thermodynamic Parameters of Metal Hydride Transfer



b. Challenges of Obtaining BDFEs in Water

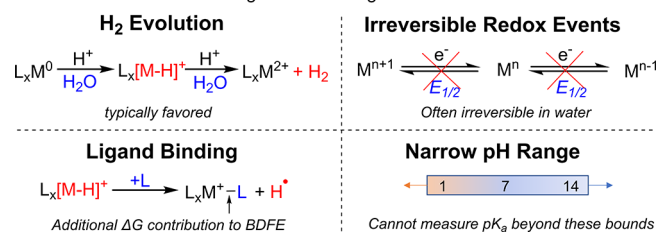


Figure 1. (a) Square scheme depicting the relationship between thermodynamic parameters of a metal hydride. (b) Challenges contributing to the difficulty of measuring BDFEs of transition metal hydrides in water.

values in organic solvents, we investigated a metal complex soluble in both MeCN and water. The desired solubility properties were achieved by adding charged functional groups, which are commonly used to engender water solubility to organometallic complexes, although they can change other thermochemical properties. Specifically, nickel complexes with two diphosphine ligands containing an amine in the backbone were singly or doubly methylated (Scheme 1). These highly charged nickel complexes enabled the study of nickel hydride BDFEs in aqueous and organic solvents.

RESULTS

Synthesis and Characterization. We synthesized charged, water-soluble derivatives of the previously reported nickel bis(diphosphine) complex, $Ni(PNP)_2^{26}$ (0-Ni) (PNP =

Et₂PCH₂NMeCH₂PEt₂), through methylation of the backbone amines (Scheme 1). Attempts to methylate the free PNP ligand resulted in a complex mixture of products, none of which could be assigned as the desired cationic ligand by ¹H and ³¹P{¹H} NMR spectroscopies. However, direct methylation of the ligand bound to a metal is precedented in related metal phosphine complexes.^{27–30}

Upon methylation with 1 or 2 equiv of methyl triflate (MeOTf), the Ni(0) complexes **1-Ni** and **2-Ni** were prepared and characterized by ¹H and ³¹P{¹H} NMR spectroscopies (where 1 and 2 refers to the nickel complex with one and two cationic ligands, respectively). **2-Ni** was further studied by single crystal X-ray crystallography and is a rare example of a structurally characterized dicationic Ni(0) complex (Figure 2). ³¹ For comparison, we also obtained a solid-state structure

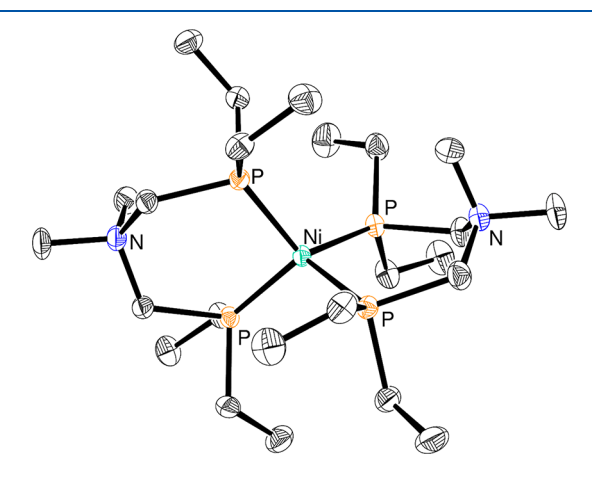


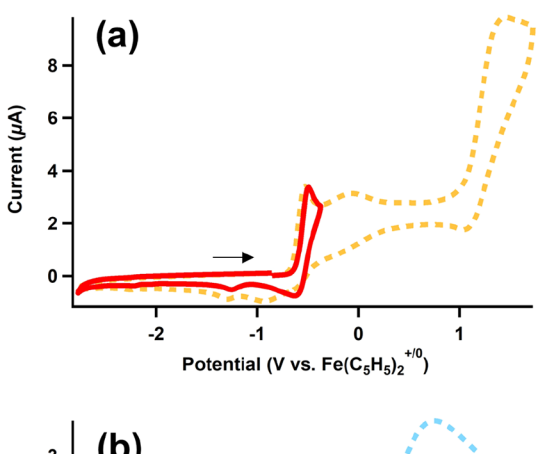
Figure 2. Solid-state structure of **2-Ni**. Thermal ellipsoids are shown at 80% level of probability. Hydrogens and outer-sphere triflate anions have been omitted for clarity.

of Ni(depp)₂ (depp = Et₂PCH₂CH₂CH₂PEt₂, Figure S1).³² The average Ni–P bond lengths (2.160(4) Å) of **2-Ni** are

Scheme 1. Synthesis of Cationic Nickel Bis(disphosphine) Complexes

similar to Ni(depp)₂ (2.148(5) Å). We also attempted methylation of [Ni(PNP)₂](BF₄)₂²⁶ to form the Ni(II) analogue of **2-Ni**, forming an overall 4+ charged complex. However, treatment of [Ni(PNP)₂](BF₄)₂ with 2 equiv of MeOTf resulted in a complex mixture of species, as determined by $^{31}P\{^{1}H\}$ NMR spectroscopy. Further attempts to isolate the Ni(I) and Ni(II) analogues of **2-Ni** through chemical oxidation of **2-Ni** were also unsuccessful (see Supporting Information). When chemical oxidation was attempted, a product was observed by ^{1}H and $^{31}P\{^{1}H\}$ NMR spectroscopies that we tentatively assign as uncoordinated ligand. (See Supporting Information).

Electrochemical Studies. 1-Ni and 2-Ni were further characterized electrochemically. All electrochemical potentials in acetonitrile (MeCN) are referenced to the $Fe(C_5H_5)_2^{+/0}$ reduction potential. Cyclic voltammetry (CV) of 2-Ni in MeCN exhibits a quasireversible Ni(I/0) redox event with an $E_{1/2} = -0.49$ V followed by an irreversible oxidation at -0.11 V that we assign as oxidation to Ni(II) (Figures 3a and S2).



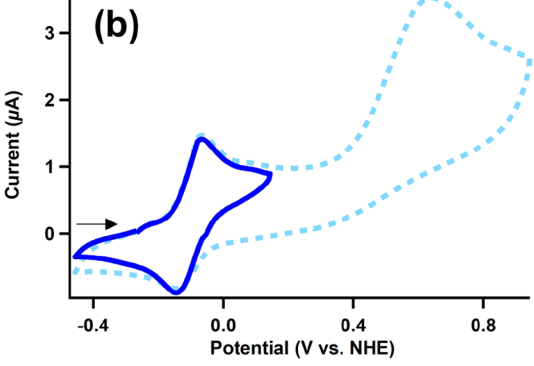


Figure 3. Cyclic voltammograms of 1 mM solutions of 2-Ni (a) in MeCN with 0.2 M TBAPF $_6$ (TBAPF $_6$ = tetrabutylammonium hexafluorophosphate) displaying the first redox feature (solid red) and a larger electrochemical potential window (orange dotted) and (b) in water with 0.1 M pH 7 phosphate buffer displaying the first redox feature (solid blue) and a larger electrochemical potential window (dashed blue). All scans were recorded at 100 mV/s.

We suspect that after oxidation to Ni(II), the cationic ligand(s) dissociate from the nickel center, followed by oxidation of a free phosphine ligand at approximately 1.1 V.^{33,34} CV of **1-Ni** in MeCN shows a reversible Ni(I/0) event at -0.82 V followed by an irreversible feature at -0.31 V assigned as the Ni(II/I) couple (Figure S3). The redox potentials of **1-Ni** and **2-Ni** follow a trend with **0-Ni**, where increasing the number of cationic ligands corresponds to more anodic reduction potentials and loss of reversibility for the Ni(II/I) couple (Table 1, Figure S4). The Ni(I/0) reduction potentials of **1-Ni** and **2-Ni** are among the most positive recorded for Ni complexes.³⁵

CV of **2-Ni** in 0.1 M pH 7 phosphate buffered water shows a reversible Ni(I/0) couple at -0.11 V versus NHE, as evidenced by the linear correlation of the square root of the scan rate with the current, and $\Delta E_{\rm p} = 70$ mV, which is near the ideal 59 mV of a one electron couple (Figures 3 and S5). This result is in contrast to the Ni(I/0) couple in MeCN, which is quasireversible. Similar to its behavior in MeCN, the Ni(II/I) couple is irreversible. **1-Ni** at pH 7 also has a reversible Ni(I/0) event followed by an irreversible event assigned to the Ni(II/I) couple (Figure S6). Insolubility of the nonmethylated compound **0-Ni** and instability of [Ni(PNP)₂](BF₄)₂ in water preclude determination of the potentials for the neutral analogue for comparison.

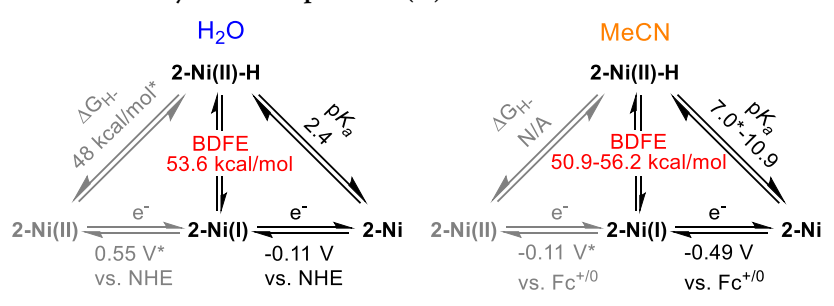
Protonation Studies. Protonation studies were performed in both MeCN and water (Scheme 1, above). Protonation of colorless 2-Ni with 4 equiv of [DMF(H)]OTf (DMF = dimethylformamide, $pK_a = 6.1^{36}$) in MeCN forms a yellow solution of 2-Ni(II)-H, which was characterized by ¹H NMR and ³¹P{¹H} NMR spectroscopic analysis. A hydride resonance was observed in the ${}^{1}H$ NMR spectrum at -15.84 ppm. The expected quintet splitting of the hydride resonance with phosphorus was not observed, even at −35 °C, despite being observed in [Ni(PNP)₂H](PF₆).²⁶ The putative hydride is unstable; decomposition is evident 10 min after [DMF(H)]OTf is added, which is as quick as we could measure the species by NMR spectroscopy. 2-Ni(II)-H fully decomposes over the course of several hours, resulting in free ligand and a paramagnetic species observable by electron paramagnetic resonance (EPR) spectroscopy (Figure S7). The EPR spectrum of this species indicates that the decomposition forms an S = 1/2 nickel-based complex. The anisotropic g factor of the paramagnetic species is greater than the g factor of a free electron (2.0023), suggesting that the signal arises from a species with more than a half full d orbital set.³⁷ Our EPR simulation does not capture all of the spectral features, which suggests that multiple paramagnetic compounds may be present. Protonation was also performed with 1 equiv of 4trifluoromethylanilium tetrafluoroborate (p $K_a = 8.03^{38}$) at -35°C, and the corresponding ¹H NMR and ³¹P{¹H} NMR spectra were taken at −35 °C. When protonating under these conditions, 2-Ni(II)-H is formed without concomitant

Table 1. Reduction Potentials of Studied Complexes in MeCN and Water

complex	$Ni(I/0)$ vs $Fe(C_5H_5)_2^{+/0}$ (V) MeCN	Ni(II/I) vs Fe(C_5H_5) ₂ ^{+/0} (V) MeCN	$Ni(I/0)$ vs NHE (V) H_2O , pH 7	Ni(II/I) vs NHE (V) H ₂ O, pH 7
0-Ni	-1.24 (rev)^{26}	-0.64 (rev)^{26}		
1-Ni	-0.82 (rev)	-0.31 (irrev)	-0.27 (rev)	0.05 (irrev)
2-Ni	-0.49 (quasi)	-0.11 (irrev)^b	-0.11 (rev)	0.55 (irrev)

^aIrreversible potentials were recorded from E_{ox} the potential at the maximum oxidative current. ^bBest assignment for this feature.

Scheme 2. Square Schemes of Nickel Hydride Complex 2-Ni(II)-H in Water and MeCN



decomposition, but decomposition begins immediately when the sample is warmed back to 25 °C (Figures S8 and S9).

Due to the instability of the hydride 2-Ni(II)—H in MeCN, a precise pK_a could not be obtained. Bounds for the pK_a were determined using acids of different pK_a values and varying concentrations as needed. Addition of 10 equiv of 4-trifluoromethylanilium tetrafluoroborate to 2-Ni consumes nearly all of the Ni(0) species, forming 2-Ni(II)—H and the decomposition product. When 1 equiv of this acid was used, incomplete reaction of 2-Ni was observed. Addition of 10 equiv of the weaker acid 4-methoxyanilinium tetrafluoroborate ($pK_a = 11.86^{38}$) to 2-Ni forms <5% of 2-Ni(II)—H and the decomposition product after 16 h. From these studies, we estimate that the pK_a is between 7.0 and 10.9 for 2-Ni(II)—H in MeCN (Figure S10). We note the possibility that the decomposition impacts the equilibrium for the reaction with the acid, and the pK_a could be lower than 7.0.

Near quantitative protonation of 2-Ni in water was achieved by dissolving the complex in a pH 1 solution of sulfuric acid, forming 2-Ni(II)-H. In H2O, a characteristic hydride resonance is present at -15.69 ppm, which is not present when D₂O is used (Figures S29 and S30). Remarkably, this hydride complex is stable in pH 1 water for over 2 weeks, and minimal decomposition is observed over ~3 months (Figures S15 and S16). The p K_a of this complex in water was measured to be 2.4 by monitoring the relative concentration of 2-Ni and **2-Ni(II)**—H with ${}^{31}P{}^{1}H{}$ NMR spectroscopy in pH 2.8 or pH 3.6 citric acid-sodium citrate buffered water (Tables S1 and S2, Figures S11-S14). The sample was monitored for 36 h to ensure that equilibrium was achieved (Figure S10). The ¹H NMR spectra taken in pH 1 water (made with sulfuric acid) have the same resonances as the citric acid-sodium citrate buffer, indicating that citrate or HSO_4^- does not coordinate the resultant hydride species.

The protonation reactivity of **1-Ni** is complicated due to two possible sites of protonation—at the metal or backbone amine—and the tendency of the compound to decompose into the homoleptic complexes **0-Ni** and **2-Ni** in solution. The pK_a of the amine in $[Ni(PNP)_2](BF_4)_2$ was previously measured to be 10.6 ± 0.1 in MeCN. Upon treatment of **1-Ni** with acid in MeCN, multiple hydride species are observed and can be assigned as $[Ni(PNP)_2H](PF_6)$, ²⁶ **2-Ni(II)—H** and presumably the nickel hydride complex of **1-Ni**. These species are likely formed through ligand exchange, rather than demethylation of the ligand backbone. Due to this ligand exchange, the pK_a could not be accurately determined in MeCN. Protonation of **1-Ni** in water was also difficult to study due to pH-dependent solubility. The aqueous pK_a value of **0-Ni** could not be determined because it is not water-soluble.

BDFE Determination. With both redox potential and pK_a data in hand, the BDFE of the Ni-H bond of **2-Ni(II)**-H was

calculated using eq 1, where E° is the $E_{1/2}$ of the Ni(I/0) reduction potential, the p $K_{\rm a}$ is the p $K_{\rm a}$ of 2-Ni(II)-H, and $\Delta G_{\rm c}^{\circ}$ is a solvent-dependent constant (52.8 kcal/mol for water³⁹ and 52.6 kcal/mol for MeCN).⁴⁰ The calculated BDFEs for 2-Ni(II)-H in water and MeCN are 53.6 and 50.9-56.2 kcal/mol, respectively (Scheme 2).

$$\Delta G_{H \bullet}^{\circ} = 1.37(pK_a) + 23.06(E^{\circ}) + \Delta G_c^{\circ}$$
 (1)

DISCUSSION

We prepared new highly charged complexes 1-Ni and 2-Ni through a post-metalation methylation procedure, which selectively methylated the backbone amines of the ligand. Cationic phosphine ligands are relatively rare in the literature and in most cases impart significantly different properties on the complex compared to their neutral analogues. The same is true for the cationic PNP ligands prepared in this work, which result in very electron-poor metal centers, making them weaker hydride donors. Unfortunately, the highly positive nature of these ligands makes it difficult to form the more electron-deficient Ni(I) and Ni(II) complexes of 1-Ni and 2-Ni. The ligands also seem to be susceptible to dissociation, as protonation experiments in MeCN show evidence of what we tentatively assign as free ligand, which is also evident in chemical oxidation experiments.

The cationic ligands result in significant anodic shifts to the redox potentials of the nickel center relative to the neutral analogue. Since there is only a single methylene spacer between the cation and the donor phosphorus atoms, we would expect significant inductive effects reducing the donor strength of the ligand. The Ni(I/0) reduction potential of 2-Ni in MeCN (-0.49~V) is very similar to a calculated reduction potential of a P_2N_2 -type Ni(0) bis(diphosphine) complex (-0.51~V) with two protons attached to the backbone pendant amines.

The tricationic nickel hydride complex 2-Ni(II)—H was synthesized in situ via protonation of 2-Ni. The anodic shift in potential from the cationic ligands is expected to result in a poorer hydride donor. As a result, protonation to form H2 is likely unfavorable. 43 The 2-Ni(II)—H complex is less stable in MeCN, leading to paramagnetic species and free ligand. As water has a higher dielectric constant, we hypothesize that it stabilizes the highly charged 2-Ni(II)-H species better than MeCN. The trends observed in the reduction potential and electrochemical reversibility are also consistent with this hypothesis. As more charged ligands are introduced, the reversibility of the Ni(I/0) and Ni(II/I) couples decreased in MeCN, suggesting that the chemical events of ligand dissociation become more favorable with more cationic ligands. However, in water, the Ni(I/0) couple remains reversible.

The p K_a range of **2-Ni** (7.0–10.9) in MeCN is significantly lower than the previously reported p K_a value of **0-Ni** (22.2), which is not surprising given its higher cationic charge. The ligand acidity method of Morris has been previously used to calculate p K_a values of metal hydrides. This method could not be used to predict a p K_a value of **2-Ni**(II)–H—which has an overall charge of 3+—because the equation of this method only accommodates hydrides with overall charges of 0, 1+, or 2+.

The stability of 2-Ni(II)-H in water allowed for the measurement of its aqueous BDFE, which is a very rare example of a transition metal hydride BDFE measured in water. This BDFE of 53.6 kcal/mol is in the range of most measured transition metal hydrides in organic solvents (typically between 50 and 60 kcal/mol). 10 Due to the necessity of using a pKa bracket, only a BDFE range of 50.9-56.2 kcal/mol could be obtained in MeCN. The measured BDFEs of 53.6 and 50.9-56.2 kcal/mol in water and MeCN, respectively, are very similar. This result is consistent with BDFEs of O-H and N-H bonds measured in multiple solvents; there is very little solvent dependence.¹⁸ Since the BDFE is within the typical range for transition metal hydrides, there appears to be little or no perturbation of the bond strength either from the water solvent or from the proximally located charges. Interestingly, the BDFE of the analogous neutral hydride [Ni(PNP)₂H](PF₆) is 54.4 kcal/ mol, approximately the same as the tricationic complex 2-Ni(II)-H.

The hydricity values for 1-Ni and 2-Ni could not be rigorously determined in aqueous or organic solvent because reversible or quasireversible Ni(II/I) couples could not be obtained. Furthermore, the inaccessibility of the Ni(II) analogues of 1-Ni and 2-Ni obviated the use of H_2 equilibration to determine hydricity, as this method requires stable Ni(II) complexes. A lower bound of hydricity for 2-Ni(II)—H in water could be estimated at 35 kcal/mol because no H_2 evolution was observed in pH 1 water after 2 weeks. Alternatively, the potential-p K_a method 39,45 can be used to estimate a hydricity of 48 kcal/mol (see Figure S17 for calculation information). However, the irreversible Ni(II/I) couple limits the accuracy of this value.

CONCLUSIONS

New monocationic and dicationic nickel(0) bis(diphosphine) complexes 1-Ni and 2-Ni were synthesized and characterized by NMR spectroscopy and cyclic voltammetry. 2-Ni was further characterized by single crystal X-ray crystallography. Electrochemical studies reveal that the Ni(I/0) couples of the cationic species are significantly anodically shifted relative to the neutral analogue and are among the most positive values measured for nickel complexes. Protonation studies were used to obtain the p K_a values of the 2-Ni(II)-H species in both water and acetonitrile. The nickel hydride bond dissociation free energies for 2-Ni(II)-H were measured in water and MeCN. The BDFE value in MeCN is very similar to the value obtained in water, which is consistent with previous studies that demonstrate solvent invariance for BDFEs of O-H and N-H bonds. This work more broadly suggests that the bond strengths of transition metal hydrides are not perturbed in water, and measured BDFE values of transition metal hydrides in organic solvents would likely be similar to the BDFE of these metal hydride bonds in water. This conclusion informs

the development of transition metal hydride catalysis in aqueous conditions.

EXPERIMENTAL SECTION

General Experimental Details. All manipulations were performed under an atmosphere of N2 in a glove box or through the use of a Schlenk line. Chemicals were obtained from commercial sources without further purification, unless otherwise noted. HPLC grade water degassed under active vacuum was used for aqueous studies. Nondeuterated organic solvents were degassed by sparging with argon and then dried by passage through an alumina column under argon pressure on a solvent drying system (JC Meyer Solvent Systems) and stored over activated 3 Å molecular sieves under a N2 atmosphere. Deuterated solvents were purchased from Cambridge Isotope Laboratories, degassed by freeze-pump-thaw methods, and then dried over activated molecular sieves prior to use, with the exception of D₂O, which was stored without molecular sieves. Tetrabutylammonium hexafluorophosphate (TBAPF₆) was recrystallized from ethanol three times. PNP, ²⁶ Ni(PNP)₂, ²⁶ Ni(depp)₂, ³² [DMF(H)]-OTf,³⁶ 4-methoxyanilinium tetrafluoroborate,⁴⁶ and 4-trifluoromethylanilinium tetrafluoroborate⁴⁶ were synthesized as previously reported. NMR spectroscopic measurements were obtained on a Bruker AVANCE600 instrument. Phosphorus NMR spectroscopy samples were referenced to internal or external H₃PO₄ or were referenced to the solvent signal of the proton spectrum. pH 7 buffer was made with monobasic and dibasic sodium phosphate. pH 1 solutions were made from sulfuric acid. pH 2.77 and pH 3.62 buffered solutions were made with citric acid and sodium citrate. X-ray diffraction studies were carried out at the UCI Department of Chemistry X-ray Crystallography Facility on a Bruker SMART APEX II diffractometer. Data were collected at 133 K using Mo K α radiation ($\lambda = 0.71073$ Å). The APEX2 program package was used to determine the unit cell parameters and for data collection. The raw frame data were processed using SAINT and SADABS to yield the reflection data file. 47,48 The structures were solved using XT, and the data were refined using XL using SHELXle as a graphical user interface.4 Electrospray ionization mass spectrometry experiments were performed on a Micromass LCT at the University of California, Irvine Mass Spectrometry Facility. Electrochemical measurements were obtained on a Pine WaveDriver 10 bipotentiostat, equipped with AfterMath software. The working electrode was a glassy carbon disc with a 1 mm diameter, the counter electrode was a glassy carbon rod, a silver wire was used as a pseudo reference in organic solvents, and a saturated calomel reference electrode (SCE) in saturated KCl was used in aqueous solvent. Aqueous potentials were converted to SCE using the conversion factor of NHE = 0.244 V versus SCE. EPR spectra were taken on an X-band Bruker EMX spectrometer, outfitted with an EMX standard resonator and a Bruker PremiumX microwave bridge. EPR simulations were performed with EasySpin.⁵¹ Spectra were taken as frozen solutions. Water pH measurements were performed with a Thermo Scientific Orion Star A216 Benchtop pH/ RDO/DO meter.

Syntheses. Synthesis of 2-Ni. A thawing solution of MeOTf (81 mg, 0.50 mmol, 2.1 equiv) in benzene (5 mL) was added to a thawing, stirring solution of 0-Ni (125 mg, 0.237 mmol, 1.0 equiv) in benzene (3 mL). The solution immediately turned cloudy and was warmed to room temperature. After 20 min, the suspension was filtered, and the resulting white solid was dissolved in MeCN. The solvent was removed in vacuo to yield 2-Ni as a white solid powder (200 mg, 84% yield). The solid was dissolved in minimal MeCN, and ether was layered on top yielding crystals suitable for single crystal Xray diffraction. ¹H NMR (600 MHz, CD₃CN, 23 °C): δ 1.03 (dt, J =14.8, 7.1 Hz, 24H, CH₃), 1.60-1.74 (m, 16H, CH₂), 3.24 (s, 20H, $NCH_2P \& NCH_3$). ¹**H NMR** (600 MHz, D₂O, 23 °C): δ 1.05 (dt, J =12.2, 7.4 Hz, 24H, CH₃), 1.68–1.80 (m, 16H, CH₂), 3.35 (s, 12H, NCH₃), 3.39 (s, 8H, NCH₂P). ³¹P{¹H} NMR (203 MHz, CD₃CN, 23 °C): δ 4.72 (s). ³¹P{¹H} NMR (203 MHz, D₂O, 23 °C): δ 4.62 (s). $^{13}C\{^{1}H\}$ NMR (151 MHz, CD₃CN, 23 °C): δ 62.4, 56.5, 24.2, 8.1. **ESI-MS** m/z: calcd [2-Ni + 2H⁺] 560.3; found m/z, 560.2.

In Situ Synthesis of 2-Ni(II)–H in MeCN. Four equivalents of [DMF(H)]OTf were added to an NMR tube charged with CD₃CN (0.6 mL) and 2-Ni (10 mg, 0.012 mmol, 1.0 equiv), consuming all of 2-Ni and forming 2-Ni(II)–H (>95% conversion). ¹H NMR (600 MHz, CD₃CN, 23 °C): δ 1.14 (dt, J = 15.0, 7.7 Hz, 24H, CH₃), 1.9 (m, 8H, CH₂), 3.31 (s, 12H, NCH₃), 3.76 (s, 8H, NCH₂P), −15.86 (s, 1H, NiH). ³¹P{¹H} NMR (203 MHz, CD₃CN, 23 °C): δ 5.49.

In Situ Synthesis of **2-Ni(II)**–**H** in H_2 O. 0.5 mL of pH 1 water was added to an NMR tube charged with **2-Ni** (3.5 mg, 0.0041 mmol), forming **2-Ni(II)**–**H** (>95% conversion). ¹**H NMR** (600 MHz, H_2 O, 23 °C): δ 1.11 (dt, J = 14.0, 7.1 Hz, 24H, CH_3), 1.9–1.98 (m, 8H, CH_2), 1.99–2.08 (m, 8H, CH_2), 3.39 (s, 12H, NCH_3), 3.9 (s, 8H, NCH_2 P), -15.69 (s, 1H, NiH). ³¹**P**{ ¹**H**} **NMR** (203 MHz, H_2 O, 23 °C): δ 5.65.

Synthesis of 1-Ni. A thawing solution of MeOTf (12 mg, 0.074 mmol, 1.0 equiv) in benzene was added to a thawing, stirring solution of 0-Ni (39 mg, 0.074 mmol, 1.0 equiv) in benzene (3 mL). The solution immediately turned cloudy and was warmed to room temperature. After 20 min, the suspension was filtered, and the recovered solid was dissolved in MeCN. The MeCN solvent was removed in vacuo, and the resultant white solid was washed with minimal ether and hexanes. The remaining solvent was removed in vacuo, yielding a white solid (48 mg, 95% yield). ¹H NMR (600 MHz, CD₃CN, 23 °C): δ 1.0 (m, 24H, CH₃), 1.3–1.37 (dg, I = 15.2, 8.1 Hz, 4H, CH_2), 1.46–1.54 (dq, J = 14.4, 7.5 Hz, 4H, CH_2), 1.57– 1.68 (m, 8H, CH₂), 2.27 (s, 3H, NCH₃), 2.49 (s, 4H, NCH₂P), 3.12 (s, 4H, NCH₂P) 3.17 (s, 6H, N(CH₃)₂). ${}^{31}P{}^{1}H$ NMR (203 MHz, CD₃CN, 23 °C): δ 4.4 (t, J_{PP} = 12.1 Hz), 5.05 (t, J_{PP} = 12.1 Hz). ¹³C{¹H} NMR (151 MHz, CD₃CN, 23 °C): δ 60.3, 60.1, 55.9, 52.6, 24.6, 22.2, 8.3, 7.8. **ESI-MS** m/z: calcd [1-Ni – H⁺] 542.3; found m/zz, 542.2.

 pK_a Measurement of 2-Ni in Water. Solutions of 2-Ni (3 or 4.5 mM) buffered to a solution pH of 2.77 or 3.62 were added to an NMR tube, establishing an equilibrium between the 2-Ni and 2-Ni(II)—H species. A $^{31}P\{^{1}H\}$ NMR spectrum was acquired and the integrations of 2-Ni and 2-Ni(II)—H were noted. After 12 and 36 h, additional $^{31}P\{^{1}H\}$ NMR spectra were taken and the ratio of the signals was unchanged relative to the internal standard HNa₂PO₄.

 pK_a Bracket Measurement of 2-Ni in MeCN. To 4 mM solutions of 2-Ni in an NMR tube was added 10.0 equiv of 4-methoxyanilinium tetrafluoroborate ($pK_a = 11.86^{38}$) or 4-trifluoromethylanilinium tetrafluoroborate ($pK_a = 8.03^{38}$). A $^{31}P\{^{1}H\}$ NMR spectrum was taken, showing near complete conversion to 2-Ni(II)—H or no conversion leaving only the 2-Ni species. A bracketing study was performed with 1 equiv of different acids, but incomplete conversion of the Ni(0) species to 2-Ni(II)—H prevented the use of the 1 equiv bracket.

ASSOCIATED CONTENT

Supporting Information

The Supporting Information is available free of charge at https://pubs.acs.org/doi/10.1021/acs.organomet.2c00319.

Experimental details, attempted chemical oxidation attempts, electrochemical data, NMR and EPR spectra, and CCDC deposition numbers: 2181764 and 2181765 (PDF)

Accession Codes

CCDC 2181764–2181765 contain the supplementary crystallographic data for this paper. These data can be obtained free of charge via www.ccdc.cam.ac.uk/data_request/cif, or by emailing data_request/cif, or by contacting The Cambridge Crystallographic Data Centre, 12 Union Road, Cambridge CB2 1EZ, UK; fax: +44 1223 336033.

AUTHOR INFORMATION

Corresponding Author

Jenny Y. Yang — Department of Chemistry, University of California, Irvine, California 92697, United States; Physical Sciences Division, Physical and Computational Sciences Directorate, Pacific Northwest National Laboratory, Richland, Washington 99354, United States; orcid.org/0000-0002-9680-8260; Email: j.yang@uci.edu

Authors

Andrew D. Cypcar — Department of Chemistry, University of California, Irvine, California 92697, United States

Tyler A. Kerr — Department of Chemistry, University of California, Irvine, California 92697, United States;

orcid.org/0000-0002-0369-4883

Complete contact information is available at: https://pubs.acs.org/10.1021/acs.organomet.2c00319

Notes

The authors declare no competing financial interest.

ACKNOWLEDGMENTS

We acknowledge NSF award # 2102589 for supporting this research. We thank Meghen Goulet from Prof. Borovik's group (UCI) for EPR assistance, Dr. Kelsey Collins for EPR simulation assistance, and Felix Grun (UCI) for mass spectrometry data collection. We also thank Dr. Nadia Léonard for helpful discussions.

REFERENCES

- (1) Morris, R. H. Hydride Complexes of the Transition Metals. *Encycl. Inorg. Bioinorg. Chem.* **2018**, 1–12.
- (2) Barlow, J. M.; Yang, J. Y. Thermodynamic Considerations for Optimizing Selective CO₂ Reduction by Molecular Catalysts. *ACS Cent. Sci.* **2019**, *5*, 580–588.
- (3) Stratakes, B. M.; Wells, K. A.; Kurtz, D. A.; Castellano, F. N.; Miller, A. J. M. Photochemical $\rm H_2$ Evolution from Bis(Diphosphine)-Nickel Hydrides Enables Low-Overpotential Electrocatalysis. *J. Am. Chem. Soc.* **2021**, *143*, 21388–21401.
- (4) Wiedner, E. S.; Chambers, M. B.; Pitman, C. L.; Bullock, R. M.; Miller, A. J. M.; Appel, A. M. Thermodynamic Hydricity of Transition Metal Hydrides. *Chem. Rev.* **2016**, *116*, 8655–8692.
- (5) Brereton, K. R.; Smith, N. E.; Hazari, N.; Miller, A. J. M. Thermodynamic and Kinetic Hydricity of Transition Metal Hydrides. *Chem. Soc. Rev.* **2020**, *49*, 7929–7948.
- (6) Wang, D.; Astruc, D. The Golden Age of Transfer Hydrogenation. Chem. Rev. 2015, 115, 6621-6686.
- (7) The Handbook of Homogeneous Hydrogenation; de Vries, J. G.; Elsevier, C. J., Eds.; Wiley-VCH: Weinheim, Germany, 2007; Vol. 1–3.
- (8) Crossley, S. W. M.; Obradors, C.; Martinez, R. M.; Shenvi, R. A. Mn-, Fe-, and Co-Catalyzed Radical Hydrofunctionalizations of Olefins. *Chem. Rev.* **2016**, *116*, 8912.
- (9) Shevick, S. L.; Wilson, C. V.; Kotesova, S.; Kim, D.; Holland, P. L.; Shenvi, R. A. Catalytic Hydrogen Atom Transfer to Alkenes: A Roadmap for Metal Hydrides and Radicals. *Chem. Sci.* **2020**, *11*, 12401–12422.
- (10) Tilset, M. Organometallic Electrochemistry: Thermodynamics of Metal-Ligand Bonding. *Comprehensive Organometallic Chemistry III*, 3rd ed.; Elsevier, 2007; pp 279–305.
- (11) Morris, R. H. Brønsted-Lowry Acid Strength of Metal Hydride and Dihydrogen Complexes. *Chem. Rev.* **2016**, *116*, 8588–8654.
- (12) Connelly Robinson, S. J.; Zall, C. M.; Miller, D. L.; Linehan, J. C.; Appel, A. M. Solvent Influence on the Thermodynamics for Hydride Transfer from Bis(Diphosphine) Complexes of Nickel. *Dalton Trans.* **2016**, *45*, 10017–10023.

- (13) Tsay, C.; Livesay, B. N.; Ruelas, S.; Yang, J. Y. Solvation Effects on Transition Metal Hydricity. *J. Am. Chem. Soc.* **2015**, *137*, 14114–14121
- (14) Ceballos, B. M.; Tsay, C.; Yang, J. Y. CO₂ Reduction or HCO₂⁻ Oxidation? Solvent-Dependent Thermochemistry of a Nickel Hydride Complex. *Chem. Commun.* **2017**, *53*, 7405–7408.
- (15) Pitman, C. L.; Brereton, K. R.; Miller, A. J. M. Aqueous Hydricity of Late Metal Catalysts as a Continuum Tuned by Ligands and the Medium. *J. Am. Chem. Soc.* **2016**, *138*, 2252–2260.
- (16) Fu, X.; Wayland, B. B. Equilibrium Thermodynamic Studies in Water: Reactions of Dihydrogen with Rhodium(III) Porphyrins Relevant to Rh–Rh, Rh–H, and Rh–OH Bond Energetics. *J. Am. Chem. Soc.* **2004**, 126, 2623–2631.
- (17) Fu, X.; Wayland, B. B. Thermodynamics of Rhodium Hydride Reactions with CO, Aldehydes, and Olefins in Water: Organo-Rhodium Porphyrin Bond Dissociation Free Energies. *J. Am. Chem. Soc.* 2005, 127, 16460–16467.
- (18) Agarwal, R. G.; Coste, S. C.; Groff, B. D.; Heuer, A. M.; Noh, H.; Parada, G. A.; Wise, C. F.; Nichols, E. M.; Warren, J. J.; Mayer, J. M. Free Energies of Proton-Coupled Electron Transfer Reagents and Their Applications. *Chem. Rev.* **2021**, *122*, 1–49.
- (19) Shaughnessy, K. H. Hydrophilic Ligands and Their Application in Aqueous-Phase Metal-Catalyzed Reactions. *Chem. Rev.* **2009**, *109*, 643–710.
- (20) Léonard, N. G.; Dhaoui, R.; Chantarojsiri, T.; Yang, J. Y. Electric Fields in Catalysis: From Enzymes to Molecular Catalysts. *ACS Catal.* **2021**, *11*, 10923–10932.
- (21) Léonard, N. G.; Chantarojsiri, T.; Ziller, J. W.; Yang, J. Y. Cationic Effects on the Net Hydrogen Atom Bond Dissociation Free Energy of High-Valent Manganese Imido Complexes. *J. Am. Chem. Soc.* 2022, 144, 1503–1508.
- (22) Christopher Almquist, C.; Removski, N.; Maron, L.; Piers, W. E. Spontaneous Ammonia Activation Through Coordination-Induced Bond Weakening in Molybdenum Complexes of a Dianionic Pentadentate Ligand Platform. *Angew. Chemie Int. Ed.* **2022**, *61*, No. e202203576.
- (23) Weberg, A. B.; Murphy, R. P.; Tomson, N. C. Oriented Internal Electrostatic Fields: An Emerging Design Element in Coordination Chemistry and Catalysis. *Chem. Sci.* **2022**, *13*, 5432–5446.
- (24) Dhar, D.; Yee, G. M.; Tolman, W. B. Effects of Charged Ligand Substituents on the Properties of the Formally Copper(III)-Hydroxide ([CuOH]²⁺) Unit. *Inorg. Chem.* **2018**, *57*, 9794.
- (25) Nie, W.; Tarnopol, D. E.; McCrory, C. C. L. Enhancing a Molecular Electrocatalyst's Activity for CO₂ Reduction by Simultaneously Modulating Three Substituent Effects. *J. Am. Chem. Soc.* **2021**, *143*, 3764–3778.
- (26) Curtis, C. J.; Miedaner, A.; Ciancanelli, R.; Ellis, W. W.; Noll, B. C.; Rakowski DuBois, M. R.; DuBois, D. L. [Ni-(Et₂PCH₂NMeCH₂PEt₂)₂]²⁺ as a Functional Model for Hydrogenases. *Inorg. Chem.* **2003**, 42, 216–227.
- (27) Redin, K.; Wilson, A. D.; Newell, R.; DuBois, M. R.; DuBois, D. L. Studies of Structural Effects on the Half-Wave Potentials of Mononuclear and Dinuclear Nickel(II) Diphosphine/Dithiolate Complexes. *Inorg. Chem.* **2007**, *46*, 1268–1276.
- (28) Kang, P.; Meyer, T. J.; Brookhart, M. Selective Electrocatalytic Reduction of Carbon Dioxide to Formate by a Water-Soluble Iridium Pincer Catalyst. *Chem. Sci.* **2013**, *4*, 3497–3502.
- (29) Klug, C. M.; Dougherty, W. G.; Kassel, W. S.; Wiedner, E. S. Electrocatalytic Hydrogen Production by a Nickel Complex Containing a Tetradentate Phosphine Ligand. *Organometallics* **2019**, 38, 1269–1279.
- (30) Erickson, J. D.; Preston, A. Z.; Linehan, J. C.; Wiedner, E. S. Enhanced Hydrogenation of Carbon Dioxide to Methanol by a Ruthenium Complex with a Charged Outer-Coordination Sphere. *ACS Catal.* **2020**, *10*, 7419–7423.
- (31) After an extensive literature search, we could find no other examples.

- (32) (a) Gordon, A. J.; Ford, R. A. The Chemist's Companion; Wiley: New York, 1972; p 436. (b) Fieser, L. F.; Fieser, M. Reagents for Organic Synthesis; Wiley: New York, 1967; Vol. 1, p 739.
- (33) Gu, L.; Wolf, L. M.; Zieliński, A.; Thiel, W.; Alcarazo, M. α -Dicationic Chelating Phosphines: Synthesis and Application to the Hydroarylation of Dienes. *J. Am. Chem. Soc.* **2017**, *139*, 4948–4953.
- (34) Reichl, K. D.; Ess, D. H.; Radosevich, A. T. Catalyzing Pyramidal Inversion: Configurational Lability of P-Stereogenic Phosphines via Single Electron Oxidation. *J. Am. Chem. Soc.* **2013**, 135, 9354–9357.
- (35) Lin, Q.; Dawson, G.; Author, C.; Diao, T. Experimental Electrochemical Potentials of Nickel Complexes Tianning Diao. *Synlett* **2021**, 32, 1602–1620.
- (36) Kilgore, U. J.; Roberts, J. A. S.; Pool, D. H.; Appel, A. M.; Stewart, M. P.; DuBois, M. R.; Dougherty, W. G.; Kassel, W. S.; Bullock, R. M.; DuBois, D. L. [Ni(PPh₂NC₆H₄X₂)₂]²⁺ Complexes as Electrocatalysts for H₂ Production: Effect of Substituents, Acids, and Water on Catalytic Rates. J. Am. Chem. Soc. **2011**, 133, 5861–5872.
- (37) Lin, C. Y.; Power, P. P. Complexes of Ni(I): A "Rare" Oxidation State of Growing Importance. *Chem. Soc. Rev.* **2017**, *46*, 5347–5399.
- (38) Kaljurand, I.; Kütt, A.; Sooväli, L.; Rodima, T.; Mäemets, V.; Leito, I.; Koppel, I. A. Extension of the Self-Consistent Spectrophotometric Basicity Scale in Acetonitrile to a Full Span of 28 pK_a Units: Unification of Different Basicity Scales. *J. Org. Chem.* **2005**, *70*, 1019–1028
- (39) Connelly, S. J.; Wiedner, E. S.; Appel, A. M. Predicting the Reactivity of Hydride Donors in Water: Thermodynamic Constants for Hydrogen. *Dalton Trans.* **2015**, *44*, 5933–5938.
- (40) Wise, C. F.; Agarwal, R. G.; Mayer, J. M. Determining Proton-Coupled Standard Potentials and X-H Bond Dissociation Free Energies in Nonaqueous Solvents Using Open-Circuit Potential Measurements. J. Am. Chem. Soc. 2020, 142, 10681–10691.
- (41) Mohr, B.; Lynn, D. M.; Grubbs, R. H. Synthesis of Water-Soluble, Aliphatic Phosphines and Their Application to Well-Defined Ruthenium Olefin Metathesis Catalysts. *Organometallics* **1996**, *15*, 4317–4325.
- (42) Horvath, S.; Fernandez, L. E.; Appel, A. M.; Hammes-Schiffer, S. pH-Dependent Reduction Potentials and Proton-Coupled Electron Transfer Mechanisms in Hydrogen-Producing Nickel Molecular Electrocatalysts. *Inorg. Chem.* **2013**, *52*, 3643–3652.
- (43) Ceballos, B. M.; Yang, J. Y. Directing the Reactivity of Metal Hydrides for Selective CO₂ Reduction. *Proc. Natl. Acad. Sci. U.S.A.* **2018**, *115*, 12686–12691.
- (44) Morris, R. H. Estimating the Acidity of Transition Metal Hydride and Dihydrogen Complexes by Adding Ligand Acidity Constants. *J. Am. Chem. Soc.* **2014**, *136*, 1948–1959.
- (45) Berning, D. E.; Noll, B. C.; DuBois, D. L. Relative Hydride, Proton, and Hydrogen Atom Transfer Abilities of [HM-(Diphosphine)₂]PF₆ Complexes (M) Pt, Ni). *J. Am. Chem. Soc.* **1999**, 121, 11432–11447.
- (46) McCarthy, B. D.; Martin, D. J.; Rountree, E. S.; Ullman, A. C.; Dempsey, J. L. Electrochemical Reduction of Brønsted Acids by Glassy Carbon in Acetonitrile: Implications for Electrocatalytic Hydrogen Evolution. *Inorg. Chem.* **2014**, *53*, 8350–8361.
- (47) Bruker. SAINT, V8.34A; Bruker AXS. Inc.: Madison, Wisconsin, USA.
- (48) Krause, L.; Herbst-Irmer, R.; Sheldrick, G. M.; Stalke, D. Comparison of Silver and Molybdenum Microfocus X-Ray Sources for Single-Crystal Structure Determination. *J. Appl. Crystallogr.* **2015**, 48, 3–10.
- (49) Sheldrick, G. M. IUCr. SHELXT Integrated Space-Group and Crystal-Structure Determination. *Acta Cryst.* **2015**, *A71*, 3–8.
- (50) Sheldrick, G. M. Crystal Structure Refinement with SHELXL. *Acta Crystallogr.* **2015**, *71*, 3–8.
- (51) Stoll, S.; Schweiger, A. EasySpin, a Comprehensive Software Package for Spectral Simulation and Analysis in EPR. *J. Magn. Reson.* **2006**, *178*, 42–55.